Global phase portraits
of quintic reversible uniform isochronous centers

Lina Guo[✉1] and Aiyong Chen[2]

[1]School of Mathematics and Statistics, Henan University of Science and Technology,
Luoyang, 471023, China
[2]Department of Mathematics, Hunan First Normal University, Changsha, 410205, China

Abstract. This paper studies the global phase portraits of uniform isochronous quintic centers at the origin with time reversibility such that their nonlinear part is not homogeneous. By using Poincaré compactification, we obtain all possible phase portraits of this quintic polynomial differential system.

Keywords: quintic polynomial system, uniform isochronous centers, global phase portraits, time reversibility.

2020 Mathematics Subject Classification: 35C15, 35Q51.

1 Introduction

In the qualitative theory of planar differential systems, one of the classical problems is to study the global phase portraits of polynomial differential systems. The global phase portraits of polynomial differential systems have been extensively investigated, see for example [7, 9, 11, 20–27].

The isochronous center's interest started the works of Huygens [15]. The isochronicity phenomena occurred in many physical problems [10]. In the past few decades the study of isochronicity, specially in the case of polynomial differential systems, has been driven by the diffusion of more powerful methods of computerized analysis [1, 8, 13, 16, 28].

We assume that p is a center, then p is a *uniform isochronous center* if the system, in polar coordinates $x = r \cos \theta, y = r \sin \theta$, is of the form $\dot{r} = G(\theta, r), \dot{\theta} = k, k \in \mathbb{R} \backslash \{0\}$. That is, the angular velocity of the orbits of an uniform isochronous center does not depend on the radius [13].

Proposition 1.1. *Assume that a planar differential polynomial system $\dot{x} = P(x, y), \dot{y} = Q(x, y)$ of degree n has a center at the origin of coordinates. Then, this center is uniform isochronous if and only if by doing a linear change of variables and a rescaling of time it can be written into the form*

$$\dot{x} = -y + xf(x, y), \qquad \dot{y} = x + yf(x, y). \tag{1.1}$$

Where $f(x, y)$ is a polynomial in x and y of degree $n - 1$, and $f(0, 0) = 0$.

✉Corresponding author. Email: 9906193@haust.edu.cn

See for instance [18] for a proof of Proposition 1.1.

Recently, the global phase portraits of differential systems with uniform isochronous centers has attracted scholars' attention, for example [2, 8, 12, 17–19]. In 1999, Chavarriga et al. study the phase portraits of the quadratic polynomial differential system S_2 at P_{33} of [8]. Collins [12] found that differential systems with uniform isochronous cubic centers may have three global different portraits. In 2016, Itikawa and Llibre [19] study the phase portraits of uniform isochronous quartic centers. The first studies on some of these phase portraits are due to Algaba et al. [3]. The phase portraits of uniform isochronous quartic centers whose nonlinear part is homogeneous and not homogeneous were studied in [19] and [18], respectively. However, there are some mistakes in [18], which are corrected in [5]. Until now there are few results about the global phase portraits of differential system with uniform isochronous of degree 5 [2]. In this paper, we will study the global phase portraits of uniform isochronous quintic centers at the origin with time reversibility such that their nonlinear part is not homogeneous. We say that systems (1.1) reversible with respect to the y-axis if it is invariant under the transformation $(x, y, t) \mapsto (-x, y, -t)$. For this case, the differential system (1.1) of quintic reversible uniform isochronous centers can be written as

$$\begin{cases} \frac{dx}{dt} = -y + x(a_1x + a_2xy + a_3x^3 + a_4xy^2 + a_5xy^3 + a_6x^3y), \\ \frac{dy}{dt} = x + y(a_1x + a_2xy + a_3x^3 + a_4xy^2 + a_5xy^3 + a_6x^3y), \end{cases} \quad (1.2)$$

where $a_i \in \mathbb{R}$, $i = 1, 2, 3, 4, 5, 6$, with $a_1^2 + a_2^2 + a_3^2 + a_4^2 \neq 0$ and $a_5^2 + a_6^2 \neq 0$.

If $a_3 \neq 0$, by a scaling $(x, y) \to \left(a_3^{-1/3}x, a_3^{-1/3}y\right)$, we can assume $a_3 = 1$, then system (1.2) becomes

$$\begin{cases} \frac{dx}{dt} = -y + x(a_1x + a_2xy + x^3 + a_4xy^2 + a_5xy^3 + a_6x^3y), \\ \frac{dy}{dt} = x + y(a_1x + a_2xy + x^3 + a_4xy^2 + a_5xy^3 + a_6x^3y). \end{cases} \quad (1.3)$$

And if $a_3 = 0$, then system (1.2) becomes

$$\begin{cases} \frac{dx}{dt} = -y + x(a_1x + a_2xy + a_4xy^2 + a_5xy^3 + a_6x^3y), \\ \frac{dy}{dt} = x + y(a_1x + a_2xy + a_4xy^2 + a_5xy^3 + a_6x^3y). \end{cases} \quad (1.4)$$

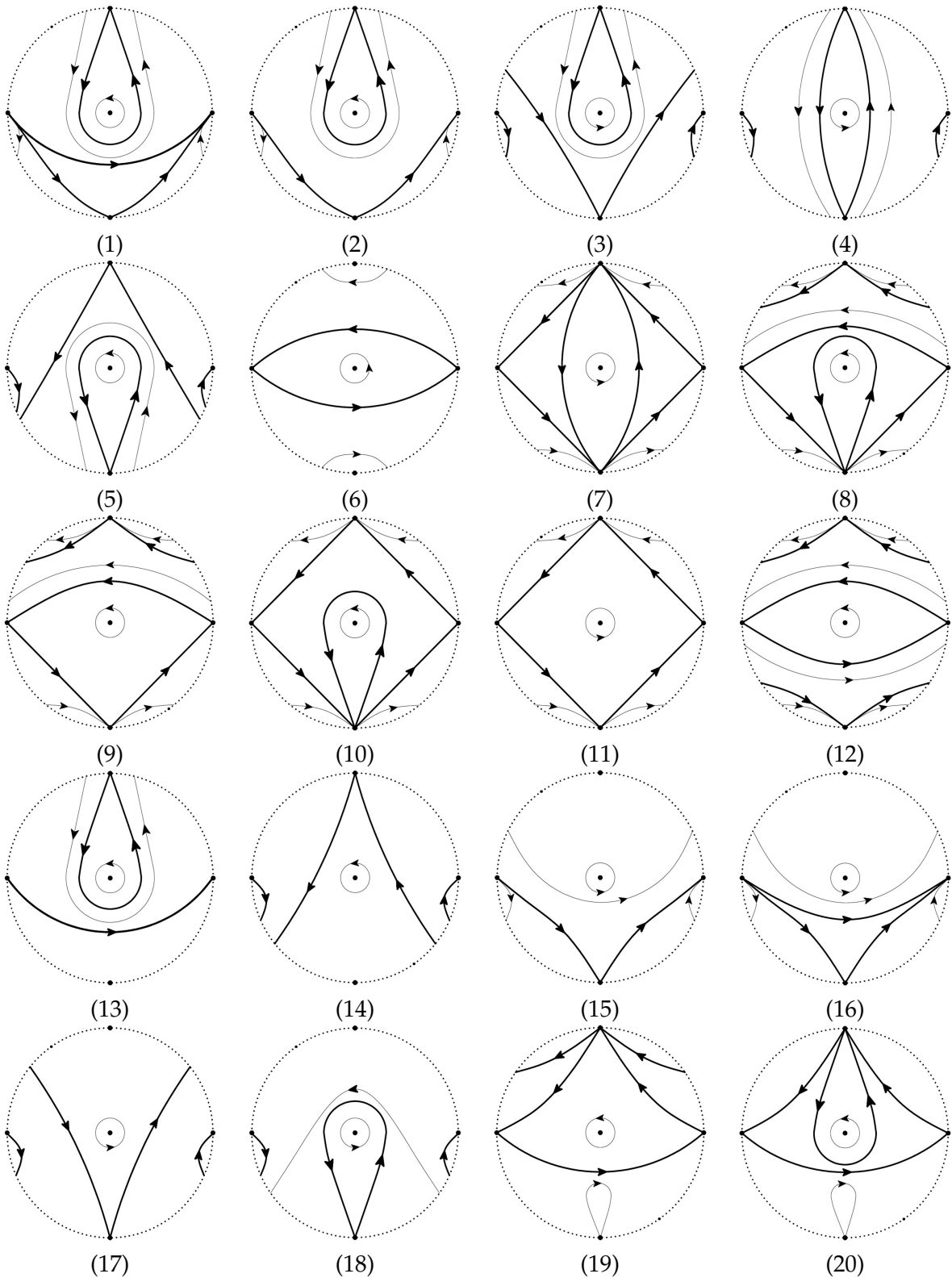In what follows we state our main results.

Theorem 1.2. *The phase portrait in the Poincaré disk of uniform isochronous quintic centers with time reversibility is topologically equivalent to one of the following 67 possibilities global phase portraits of Figure 1.1.*
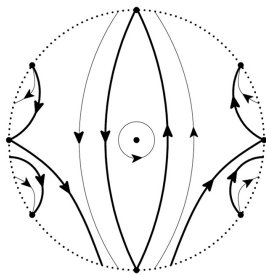
The rest of this paper is organized as follows. In Section 2, we characterize the global phase portraits of system (1.2) in the Poincaré disc, that is we prove Theorem 1.2.
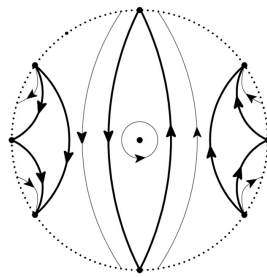
2   Proof of the results

In this section, we will prove Theorem 1.2. In order to obtain all possible phase portraits in the Poincaré disc for the uniform isochronous system of degree 5, we shall study the finite and infinite singular points of system (1.2).

By discussing the coefficient a_3 of system (1.2), we divide into the following two cases: if $a_3 \neq 0$, by parameter and time scale transformation, the system (1.2) can be given by system (1.3); if $a_3 = 0$, the system (1.2) can be given by system (1.4). Next, we will study the phase portraits of system (1.3) and system (1.4).
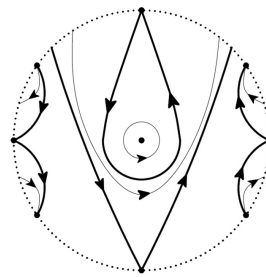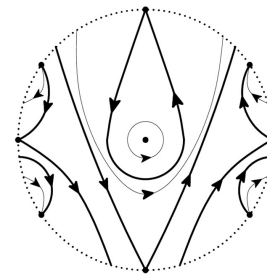
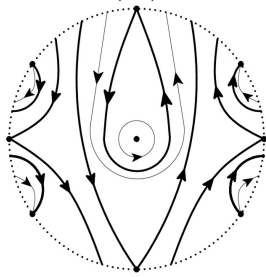(1)　　　　(2)　　　　(3)　　　　(4)

(5)　　　　(6)　　　　(7)　　　　(8)

(9)　　　　(10)　　　　(11)　　　　(12)

(13)　　　　(14)　　　　(15)　　　　(16)

(17)　　　　(18)　　　　(19)　　　　(20)

(21)

(22)

(23)

(24)

(25)

(26)

(27)

(28)

(29)

(30)

(31)

(32)

(33)

(34)

(35)

(36)

(37)

(38)

(39)

(40)

(41) (42) (43) (44)
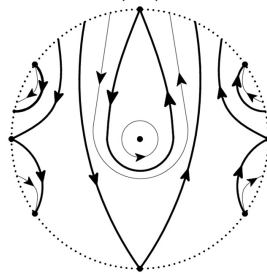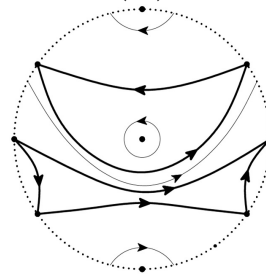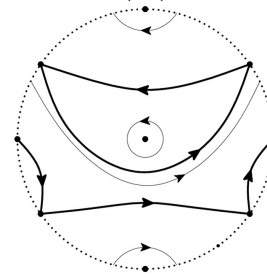
(45) (46) (47) (48)
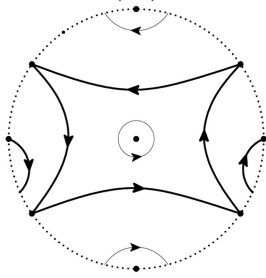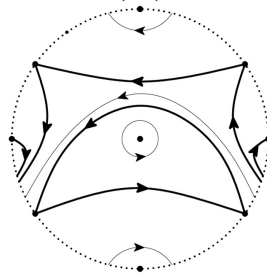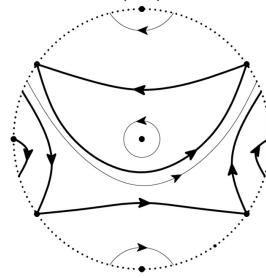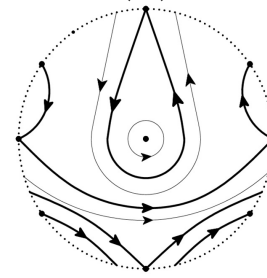
(49) (50) (51) (52)
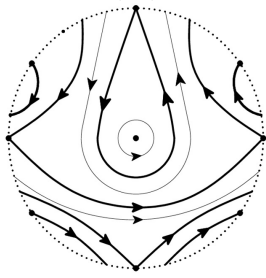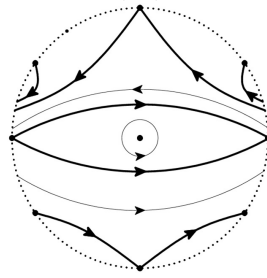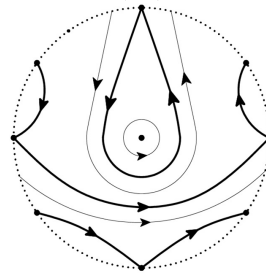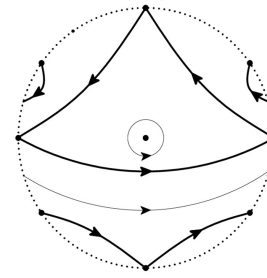
(53) (54) (55) (56)
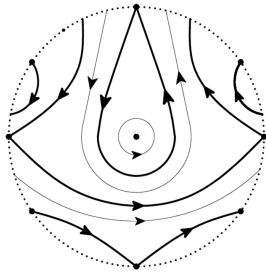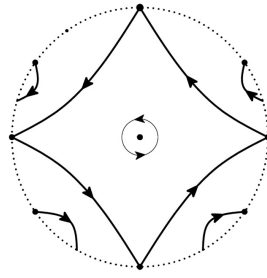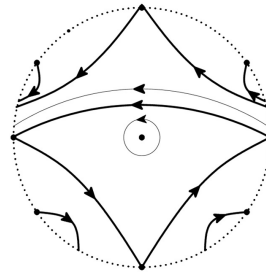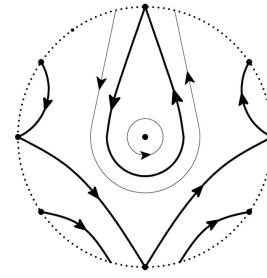
(57) (58) (59) (60)
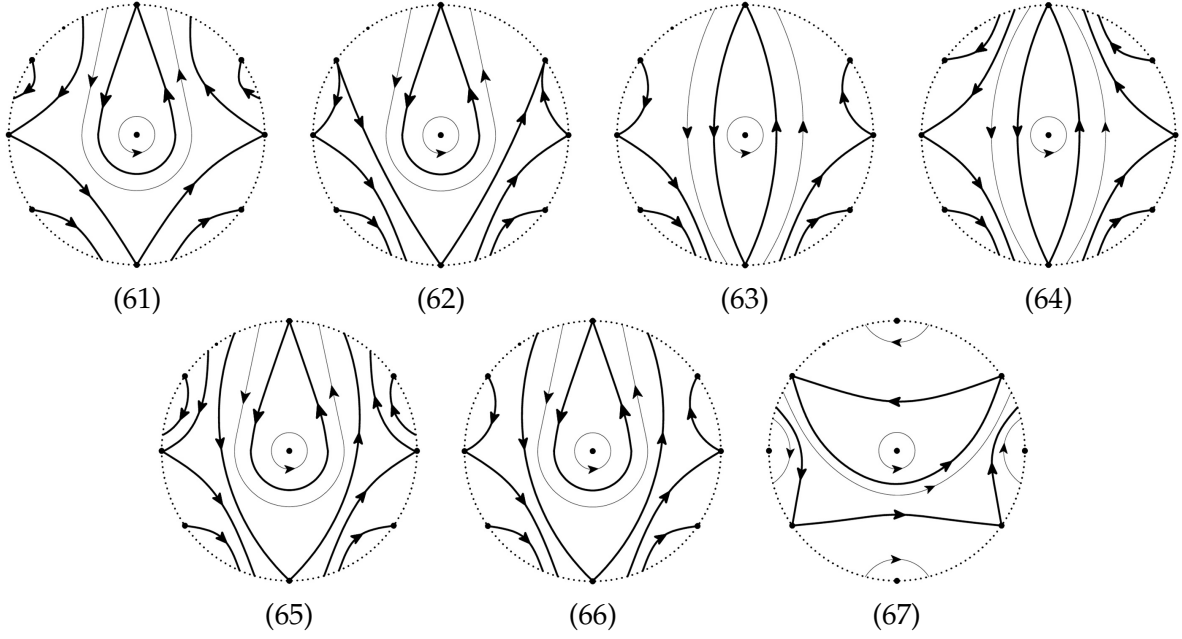
Figure 1.1: Global phase portraits of system (1.2)

Table 1.1: The corresponding relationship between the global phase portraits of system (1.3) and Figure 1.1

Figure 1.1	System (1.3)
(1)–(5)	$a_6 = 0$, $a_5 > 0$;
	$a_5 = 0$, $a_6 > 0$, $a_4 = 0$;
	$a_5 a_6 > 0$, $a_5 > 0$.
(6)	$a_6 = 0$, $a_5 < 0$;
	$a_5 = 0$, $a_6 < 0$, $a_4 = 0$, $a_6 < -a_2{}^2/4$;
	$a_5 a_6 > 0$, $a_6 < 0$.
(7)–(12)	$a_5 = 0$, $-a_2{}^2/4 \leq a_6 < 0$, $a_4 = 0$.
(13)–(14)	$a_5 = 0$, $a_6 > 0$, $a_4 > 0$.
(15)–(18)	$a_5 = 0$, $a_6 > 0$, $a_4 < 0$.
(19)–(21)	$a_5 = 0$, $a_6 < 0$, $a_4 \neq 0$.
(25)–(30)	$a_4 a_6 - a_5 = 0$, $a_5 a_6 < 0$, $a_6 < 0$, $4(a_5 - a_6) \geq a_2{}^2$.
(31)–(46)	$a_4 a_6 - a_5 = 0$, $a_5 a_6 < 0$, $a_6 < 0$, $a_2 \neq 0$, $4(a_5 - a_6) < a_2{}^2$.
(47)–(51)	$a_4 a_6 - a_5 = 0$, $a_5 a_6 < 0$, $a_6 > 0$;
	$a_4 a_6 - a_5 \neq 0$, $a_5 a_6 < 0$, $a_6 > 0$.
(52)–(66)	$a_4 a_6 - a_5 \neq 0$, $a_5 a_6 < 0$, $a_6 < 0$.

In polar coordinates defined by $(x, y) = (r \cos \theta, r \sin \theta)$, a planar differential system (1.2) with an uniform isochronous center at the origin always can be written as $\dot{r} = p(r, \theta), \dot{\theta} = 1$. Hence such systems have no finite points except the origin.

By using Poincaré compactification in [14], in the local chart U_1, we obtain

$$\begin{cases} \dot{u} = (1 + u^2)v^4, \\ \dot{v} = (uv^4 - a_1 v^3 - a_2 u v^3 - a_3 v - a_4 u^2 v - a_5 u^3 - a_6 u)v, \end{cases} \tag{2.1}$$

Table 1.2: The corresponding relationship between the global phase portraits of system (1.4) and Figure 1.1

Figure 1.1	System (1.4)
(1)–(5)	$a_5 = 0, \ a_6 > 0.$
(6)	$a_5 = 0, \ a_6 < -a_2{}^2/4;$
	$a_5 a_6 > 0.$
(7)–(12)	$a_5 = 0, \ -a_2{}^2/4 \leq a_6 < 0, \ a_4 = 0.$
(19)–(21)	$a_5 = 0, \ a_6 < 0, \ a_4 \neq 0.$
(22)	$a_5 a_6 > 0, \ a_6 > 0.$
(23)–(24)	$a_5 = 0, \ a_6 > 0, \ a_4 \neq 0.$
(25)–(30)	$a_4 = 0, \ a_5 a_6 < 0, \ a_6 < 0, \ 4(a_5 - a_6) \geq a_2{}^2.$
(31)–(46)	$a_4 = 0, \ a_5 a_6 < 0, \ a_6 < 0, \ a_2 \neq 0, \ 4(a_5 - a_6) < a_2{}^2.$
(52)–(66)	$a_5 a_6 < 0, \ a_6 < 0, \ a_4 \neq 0.$
(29), (67)	$a_5 a_6 < 0, \ a_6 > 0, \ a_4 \neq 0;$
	$a_5 a_6 < 0, \ a_6 > 0, \ a_4 = 0.$

and therefore all the points $(u, 0)$ for all $u \in \mathbb{R}$ are infinite singular points of the system (2.1) in U_1. In order to obtain the local phase portraits near the infinity, we make a transformation $\mathrm{d}s = v\mathrm{d}t$ and obtain the following system

$$\begin{cases} u' = (1 + u^2)v^3, \\ v' = uv^4 - a_1 v^3 - a_2 uv^3 - a_3 v - a_4 u^2 v - a_5 u^3 - a_6 u. \end{cases} \tag{2.2}$$

Where the prime denotes derivative with respect to s and the system (2.2) has infinite singular points in the u-axis.

In the local chart U_2, we obtain

$$\begin{cases} \dot{u} = -(1 + u^2)v^4, \\ \dot{v} = (-uv^4 - a_1 uv^3 - a_2 uv^2 - a_3 u^3 v - a_4 u^2 v - a_5 u - a_6 u^3)v. \end{cases} \tag{2.3}$$

After the rescaling of time $\mathrm{d}s = v\mathrm{d}t$, we obtain

$$\begin{cases} u' = -(1 + u^2)v^4, \\ v' = -uv^4 - a_1 uv^3 - a_2 uv^2 - a_3 u^3 v - a_4 u^2 v - a_5 u - a_6 u^3. \end{cases} \tag{2.4}$$

It is obvious that the system (2.4) has the only singular point $O_{u_2}(0, 0)$.

2.1 Global phase portraits of system (1.3)

In this section, we discuss the global phase portraits of system (1.3). According to the number of the singular points in the u-axis, the system can be divided into the following five cases.

Case I: $a_6 = 0$, $a_5 \neq 0$.

In the chart U_1, the system (2.2) has one singular point in the u-axis, that is $O_{U_1}(0, 0)$, the corresponding linear part of system (2.2) is

$$\begin{pmatrix} 0 & 0 \\ 0 & -1 \end{pmatrix}.$$

By the Theorem 2.19 of [14], we have the statements: if $a_5 > 0$, then $O_{U_1}(0,0)$ is a stable node; if $a_5 < 0$, then $O_{U_1}(0,0)$ is a saddle.

For chart U_2, the system (2.4) has only one singular point $O_{U_2}(0,0)$, the corresponding linear part of system (2.4) is

$$\begin{pmatrix} 0 & 0 \\ -a_5 & 0 \end{pmatrix}.$$

It is easy to find that $O_{U_2}(0,0)$ is a nilpotent singularity. By the Theorem 3.5 of [14], we have the statements: if $a_5 > 0$, then $O_{U_2}(0,0)$ is a nilpotent saddle; if $a_5 < 0$, and the system (2.4) is symmetry about v-axis, then $O_{U_2}(0,0)$ is a center. If the same situation appears again, we will not explain in detail.

By the above analysis, if $a_5 > 0$, the local phase portrait of system (1.3) is shown in Figure 2.1. Since $v'|_{v=0} = -a_5 u^3$: when $u > 0$, $v' < 0$; when $u < 0$, $v' > 0$, the direction of the local phase portrait through the disc is shown in the Figure 2.1.
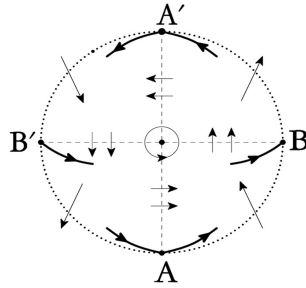
Figure 2.1: Local phase portrait of system (1.3) on the Poincaré disk of Case I for $a_5 > 0$.

In Figure 2.1, there are four singularities on the equator, i.e. A, B, A', B', and the direction between any two points is shown. Firstly, we consider the point A_1. Since the system (1.3) is symmetry about y axis, there are only four possibilities for the ω-limit set of unstable manifold: a singularity on the arc $\overset{\frown}{BA'}$, a point A, a point B, and itself (return to point A_1 after bypassing the periodic orbit around the origin, forming a homoclinic orbit). They are shown in Figure 2.2 (1)–(4).
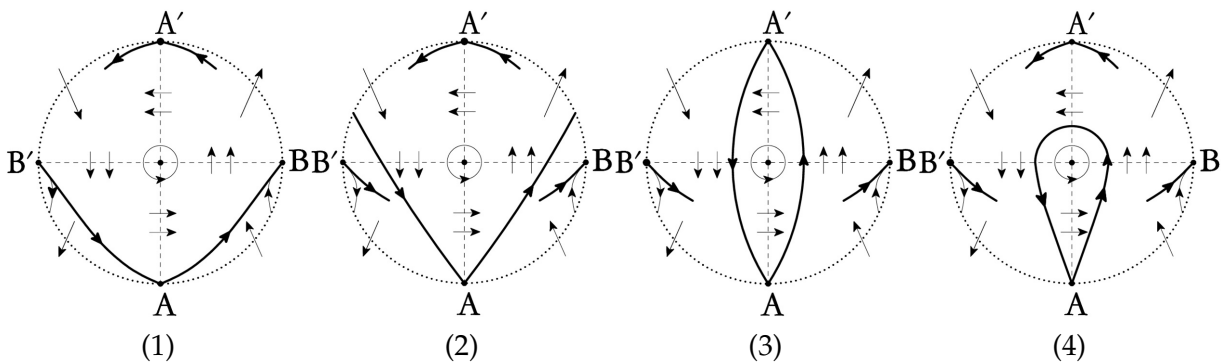
Figure 2.2: Consider the point A in Figure 2.1, four possibilities for the ω limit set of an unstable manifold.

The ω-limit set of the unstable manifold at point A' in Figure 2.2 (1) can only be itself (bypass the origin and returns to A' again, forming a homoclinic orbit). Therefore, there are

two possibility global phase portraits on the Poincaré disk, as shown in Figure 1.1 (1) and (2).

The ω-limit set of the unstable manifold at point A' in Figure 2.2 (2) can only be itself (bypass the origin and returns to A' again, forming a homoclinic orbit). Next, we consider a singular point on the arc $\overset{\frown}{AB'}$, and its α-limit set can only be a point B'. Based on the symmetry of the original system, the ω-limit set of a singular point on the arc $\overset{\frown}{AB}$ can only be a point B, and its phase portrait is equivalent to the Figure 1.1 (3).

The α-limit set of a singular point on the arc $\overset{\frown}{AB'}$ in Figure 2.2 (3) can only be the point B'. Based on the symmetry of the original system, the ω-limit set of a singular point on the arc $\overset{\frown}{AB}$ can only be the point B, its phase portrait is equivalent to the Figure 1.1 (4).

The α-limit set of the stable manifold at point A' in Figure 2.2 (4) can only be a singular point on the arc $\overset{\frown}{AB}$. Based on the symmetry of the original system, the ω-limit set of a singular point on the arc $\overset{\frown}{AB'}$ can only be the point B, and its phase portrait is equivalent to the Figure 1.1 (5).

If $a_5 < 0$, the local phase portrait of the system (1.3) on the Poincaré disk is shown in Figure 2.3, which has four singularities on its equator.
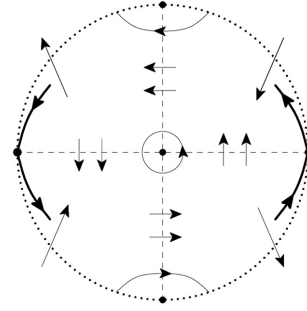

Figure 2.3: The local phase portraits of system (1.3) on the Poincaré disk of Case I for $a_5 < 0$.

By the same argument as Figure 2.1, Figure 2.3 has only one global phase portrait, as shown in the Figure 1.1 (6). This is the only one global phase portrait that can be determined. Therefore, there are 6 possible global phase portraits of system (1.3) in Case I, as shown in Figure 1.1 (1)–(6).

Case II: $a_5 = 0$, $a_6 \neq 0$.

In chart U_1, $O_{U_1}(0,0)$ is a singular point of system (2.2), and its linear part is

$$\begin{pmatrix} 0 & 0 \\ -a_6 & -1 \end{pmatrix}.$$

Applying the Theorem 2.19 of [14], we have the statements: if $a_6 > 0$, then $O_{U_1}(0,0)$ is a stable node; if $a_6 < 0$, then $O_{U_1}(0,0)$ is an unstable node.

For the chart U_2, the system (2.4) can be written as

$$\begin{cases} u' = -(1+u^2)v^3, \\ v' = -uv^4 - a_1uv^3 - a_2uv^2 - u^3v - a_4uv - a_6u^3. \end{cases} \tag{2.5}$$

The origin O_{U_2} $(0,0)$ of system (2.5) is a singular point and its linear part is identically zero, so the O_{U_2} $(0,0)$ is degenerate.

To investigate the local phase portraits of the degenerate singular points, we use the quasi-homogeneous directional blow up(or (α, β)-blow up) technique [4,6] . Since the choice of the exponents α and β depends on the coefficients a_4 of system (2.5), we need to consider whether a_4 is zero. Thus we apply a (3,2)-blow up and (1,1)-blow up to system (2.5) if $a_4 \neq 0$ and $a_4 = 0$, respectively.

Case II.1: $a_4 = 0$. When $a_4 = 0$, applying a $(1,1)$-blow up to system (2.5). Firstly, we apply blow-up $(u, v) \mapsto (\bar{u}, \bar{u}\bar{v})$ in the positive u-direction. After division by $\bar{u}^2$, we get,

$$\begin{cases} \bar{u}' = -(1 + \bar{u}^2)\bar{u}\bar{v}^3, \\ \bar{v}' = -(-\bar{v}^4 + a_1\bar{u}\bar{v}^3 + a_2\bar{v}^2 + \bar{u}\bar{v} + a_6). \end{cases} \tag{2.6}$$

Since in the line $\bar{u} = 0$, we have

$$\bar{v}^4 - a_2\bar{v}^2 - a_6 = 0.$$

Next, we only need to discuss the existence of the roots of the above equation.

(a) If $\sqrt{a_2^2 + 4a_6} > a_2$, i.e. $a_6 > 0$, the equilibrium of (2.6) are $P_1\left(0, \sqrt{\left(a_2 + \sqrt{a_2^2 + 4a_6}\right)/2}\right)$ and $P_2\left(0, -\sqrt{\left(a_2 + \sqrt{a_2^2 + 4a_6}\right)/2}\right)$. The corresponding linear part of system (3.11) at P_1 is

$$\begin{pmatrix} -\left(\sqrt{\left(a_2 + \sqrt{a_2^2 + 4a_6}\right)/2}\right)^3 & 0 \\ * & 2\sqrt{\left(a_2 + \sqrt{a_2^2 + 4a_6}\right)/2}\sqrt{a_2^2 + 4a_6} \end{pmatrix},$$

where "$*$" stands for the formula about parameters a_2 and a_6. Applying the Theorem 2.15 of [14], we have P_1 is a saddle. By the same argument, P_2 is a saddle.

(b) If $\sqrt{a_2^2 + 4a_6} < a_2$, i.e. $-a_2^2/4 < a_6 < 0, a_2 > 0$, the singular points of system (2.6) in the line $\bar{u} = 0$ are $P_1\left(0, \sqrt{\left(a_2 + \sqrt{a_2^2 + 4a_6}\right)/2}\right)$, $P_2\left(0, -\sqrt{\left(a_2 + \sqrt{a_2^2 + 4a_6}\right)/2}\right)$, $P_3\left(0, \sqrt{\left(a_2 - \sqrt{a_2^2 + 4a_6}\right)/2}\right)$ and $P_4\left(0, \sqrt{\left(a_2 - \sqrt{a_2^2 + 4a_6}\right)/2}\right)$. By the Theorem 2.15 of [14], P_1 is a saddle, P_2 is a saddle, P_3 is a stable node, and P_4 is an unstable node.

(c) If $a_2^2 + 4a_6 < 0$, i.e. $-a_2^2/4 > a_6$, then $\bar{v}^4 - a_2\bar{v}^2 - a_6 = 0$ has no roots, that is, the system (2.6) has no singular point in $\bar{v}$-axis.

(d) If $a_2^2 + 4a_6 = 0$, i.e. $-a_2^2/4 = a_6$, the singular points of system (2.6) in the line $\bar{u} = 0$ are $P_1\left(0, \sqrt{a_2/2}\right)$, $P_2\left(0, \sqrt{a_2/2}\right)$. By Theorem 3.5 of [14], P_1 is a saddle-node, and P_2 is a saddle-node.

Consider the blow-up $(u, v) \mapsto (-\bar{u}, \bar{u}\bar{v})$ in the negative u-direction. After cancelling a common factor $\bar{u}^2$, we obtain

$$\begin{cases} \bar{u}' = (1 + \bar{u}^2)\bar{u}\bar{v}^3, \\ \bar{v}' = -\bar{v}^4 + a_1\bar{u}\bar{v}^3 + a_2\bar{v}^2 + \bar{u}\bar{v} + a_6. \end{cases} \tag{2.7}$$

It can be verified that system (2.7) and system (2.6) have the same number and type of singularities.

In addition, we apply blow-up $(u, v) \mapsto (\bar{u}\bar{v}, \bar{v})$ in the positive v-direction as well as $(u, v) \mapsto (\bar{u}\bar{v}, -\bar{v})$ in the negative v-direction. After division by $\bar{v}^2$, we get, respectively,

$$\begin{cases} \bar{u}' = -1 + \bar{u}^2(a_1\bar{v} + a_2 + a_3\bar{u}^2\bar{v} + a_6\bar{u}^2), \\ \bar{v}' = -\bar{u}\bar{v}(\bar{v}^2 + a_1\bar{v} + a_2 + a_3\bar{u}^2\bar{v} + a_6\bar{u}^2), \end{cases} \tag{2.8}$$

and

$$\begin{cases} \bar{u}' = 1 + \bar{u}^2(-a_1\bar{v} + a_2 - a_3\bar{u}^2\bar{v} + a_6\bar{u}^2), \\ \bar{v}' = \bar{u}\bar{v}(\bar{v}^2 - a_1\bar{v} + a_2 - a_3\bar{u}^2\bar{v} + a_6\bar{u}^2). \end{cases} \tag{2.9}$$

It is obvious that the origin of system (2.8) and system (2.9) are not a singular point.

The blow up procedure and local phase portrait of the system (2.5) at the origin are shown in Figure 2.4 in Case (a). The trajectories of the circle is shown in Figure 2.4 (1). Retracting the circle to the origin and obtaining the trajectories in the *uov* plane near the origin, see Figure 2.4 (2). Considering the transformation $ds = vdt$, the u axis is filled with singular points, and the negative v-axis direction is reversed, as shown in Figure 2.4 (3).
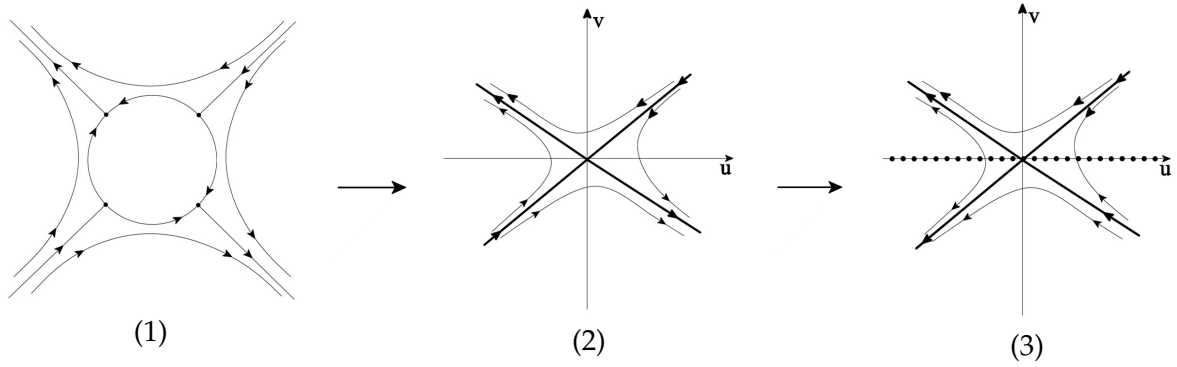
Figure 2.4: The local phase portrait of system (2.3) at the origin. The horizontal axis (3) is filled with singular points.

By the same argument as Case (a), we can obtain the local phase portrait of the system (2.5) of Case (b) and Case (d) at the origin and is shown in Figure 2.5(a). Then the local phase portrait of (1.3) of Case (a), Case (b) (d) and Case (c) are shown in Figure 2.1, Figure 2.5(b) and Figure 2.3, respectively.
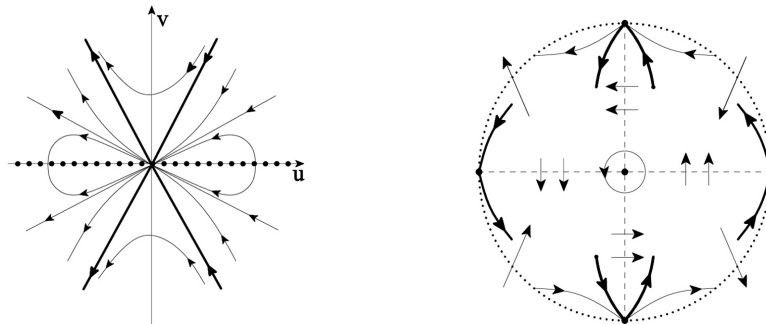
(a) The local phase portrait of the system (2.5) of Case (b) at the origin.

(b) Local phase portrait of system (1.3) on the Poincaré disk of Case (b).

Figure 2.5: Local phase portraits of systems (2.5) and (1.3).

For Case II.1, according to the symmetry and the direction through the Poincaré disk of system (1.3), we can obtain that, for Case (a), Figure 2.1 corresponds to the possible global phase portraits are Figure 1.1 (1)–(5); for Case (b) and Case (d), Figure 2.5(b) corresponds to the possible global phase portraits are Figure 1.1 (7)–(12); for Case (c), Figure 2.3 corresponds to the possible global phase portraits is Figure 1.1 (6). Therefore, there are 12 possible global phase portraits of system (1.2) of Case II.1, see Figure 1.1 (1)–(12).

Case II.2: $a_4 \neq 0$. Since $a_4 \neq 0$, applying a $(3, 2)$-blow up to system (2.5). By the same argument as Case II.1, we get the local phase portrait of system (2.5) at the origin, see Figure 2.6. Then the local phase portraits of $a_6 > 0, a_4 < 0$ and $a_6 < 0, a_4 < 0$ of the system (2.5) are topologically equivalent to (1) and (2) in Figure 2.6, respectively.

(1) $a_6 > 0, a_4 > 0$ (2) $a_6 < 0, a_4 > 0$
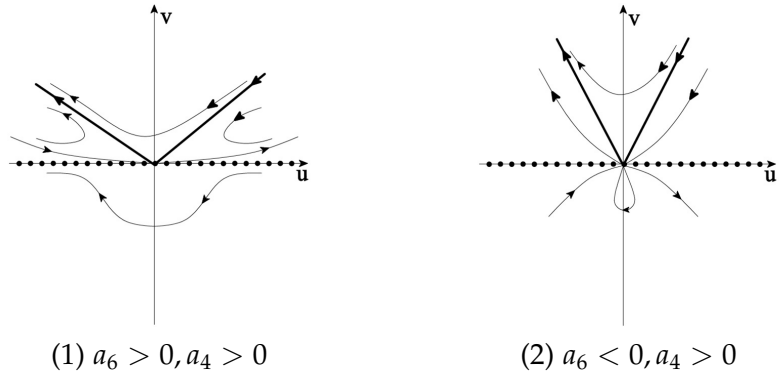
Figure 2.6: The local phase portrait of system (2.5) at the origin of Subcase II.2.

From the above analysis, we characterize the local phase portrait of system (1.3) on the Poincaré disk, see Figure 2.7 (1)–(3), and they are topologically equivalent to the possible global phase portraits Figure 1.1 (13)–(14), (15)–(18), (19)–(21) of Theorem 1.2, respectively. Therefore we can obtain the global phase portraits for Subcase II.2 shown in Figure 1.1 (13)–(21) of Theorem 1.2.

(1) $a_6 > 0, a_4 > 0$.   (2) $a_6 > 0, a_4 < 0$.   (3) $a_6 < 0$.

Figure 2.7: Local phase portrait of system (1.3) on the Poincaré disk of Subcase II.2.

Case III: $a_5 a_6 > 0$.

In the chart U_1, we consider the system (2.2). Since $a_5 a_6 > 0$, the system (2.2) has only one singular point $O_{U_1}(0, 0)$, and its linear part of system (2.2) is

$$\begin{pmatrix} 0 & 0 \\ -a_6 & -1 \end{pmatrix}.$$

Its type of singular point is the same as the Case II.

In the chart U_2, the origin is the only one singular point of system (2.4). Its linear part is

$$\begin{pmatrix} 0 & 0 \\ -a_5 & 0 \end{pmatrix}.$$

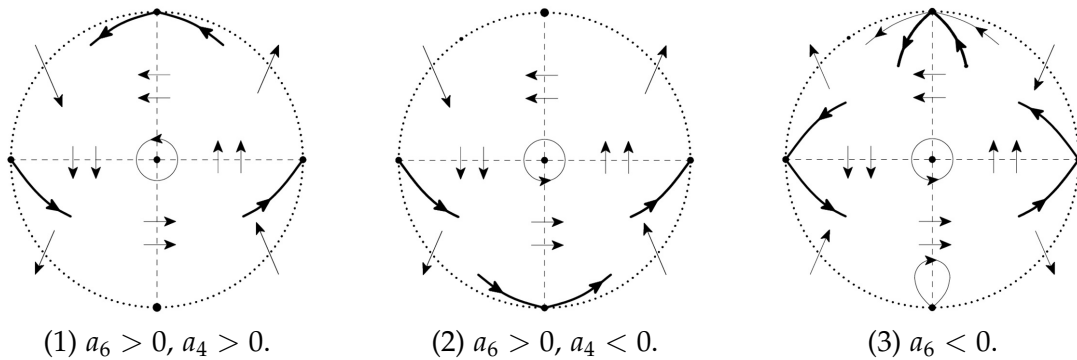Applying the Theorem 3.5 of [14], we have if $a_5 > 0$, then the origin $O_{U_2}(0,0)$ is a saddle; and if $a_5 < 0$, then $O_{U_2}(0,0)$ is a center.

According to the above analysis, we characterize the local phase portrait of system (1.3) on the Poincaré disk, see Figure 2.1 and Figure 2.3. Consequently the possible global phase portraits can referenced by Case I, that is, they are shown in Figure 1.1(1)–(6) of Theorem 1.2.

Case IV: $a_4 a_6 - a_5 = 0$, $a_5 a_6 < 0$.

In the chart U_1, we consider the system (2.2). It is easy to find that there are three singular points, $O_{U_1}(0,0)$, $P_1(\sqrt{-a_6/a_5}, 0)$ and $P_2(\sqrt{-a_6/a_5}, 0)$.

For the point $O_{U_1}(0,0)$, we have the same results as the Case II. For the points P_1 and P_2, their linear part is

$$\begin{pmatrix} 0 & 0 \\ 2a_6 & 0 \end{pmatrix}.$$

By the Theorem 3.5 of [14], if $a_6 > 0$, then P_1 and P_2 are saddles. If $a_6 < 0$,

(a) For $a_2 \neq 0$, we have the following statements hold.

(a.1) If $4(a_5 - a_6) \geq a_2^2$, then P_1 and P_2 are centers;

(a.2) If $4(a_5 - a_6) < a_2^2$, then the phase portrait of P_1 and P_2 of the system (2.2) consists of one hyperbolic and one elliptic sector.

(b) If $a_1 \neq 0$, $a_2 = 0$, and $9a_1^2 a_5 < 16 a_6 (a_6 - a_5)$, then P_1 and P_2 are centers.

(c) If $a_1 = 0$, $a_2 = 0$, and $4(a_5 - a_6) > 9$, then P_1 and P_2 are centers.

In the chart U_2, the origin $O_{U_2}(0,0)$ is the only one singular point of system (2.4). By the same argument as the Case III, we have if $a_5 > 0$, then the origin $O_{U_2}(0,0)$ is a saddle, and if $a_5 < 0$, then the origin $O_{U_2}(0,0)$ is a center.

Except Case (a.2), the local phase portraits of system (1.3) on the Poincaré disk is shown in Figure 2.8.
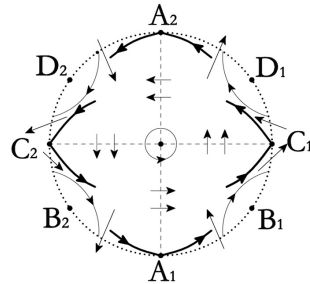

Figure 2.8: The local phase portrait of system (1.3) on the Poincaré disk except Case (a.2).

In Figure 2.8, there are eight singularities on the equator, i.e. $A_1, B_1, C_1, D_1, A_2, B_2, C_2, D_2$, and the direction between any two points is shown. Firstly, we consider the point A_1. Since the system (1.3) is symmetry about y axis, there are only five possibilities for the ω-limit set of unstable manifold: a singularity on the arc $\overarc{B_1C_1}$, a point C_1, a singular on the arc $\overarc{D_1A_2}$, a point A_2, and itself (bypass the origin and return to A_1 again, forming a homoclinic orbit). As shown in Figure 2.9 (1)–(5).
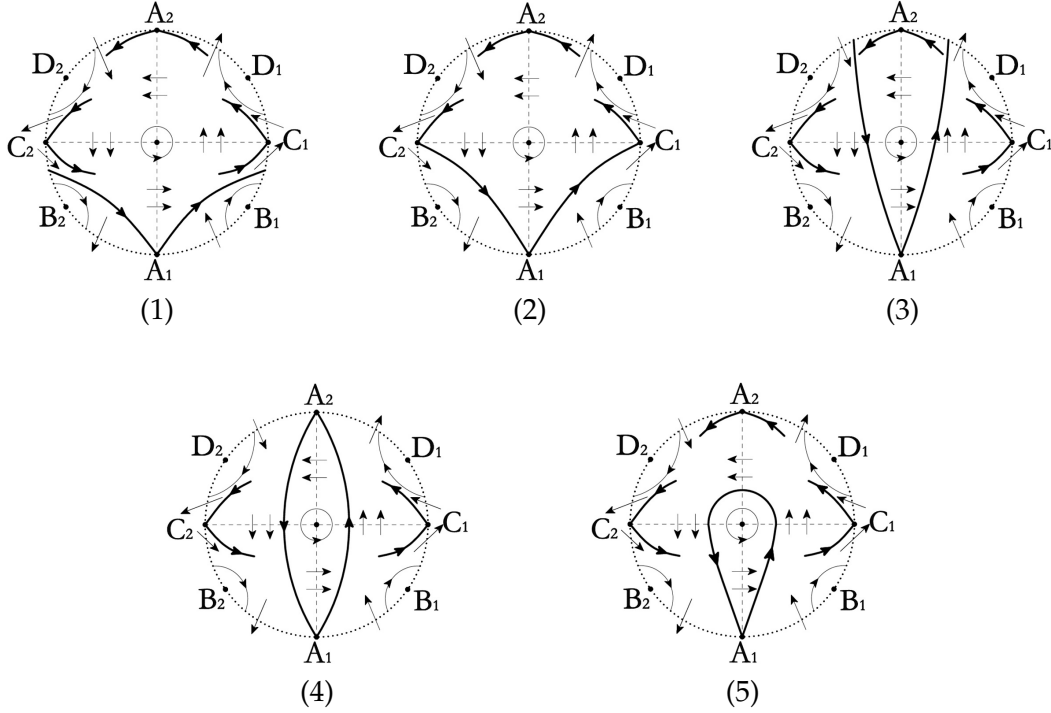

(1)   (2)   (3)

(4)   (5)

Figure 2.9: Consider the point A_1 of Figure 2.8, five possibilities for the ω-limit set of an unstable manifold at this point.

Figure 2.9 (1): Consider the point C_2, the ω-limit set of the unstable manifold at this point can only be the point C_1. Next, we consider the unstable manifold at point C_1. According to the symmetry of the original system, there are three possibilities for the ω-limit set of an unstable manifold at the point C_1, which are a point on $\overarc{D_1A_2}$, A_2 and C_2.

When the ω-limit set of an unstable manifold at point C_1 is a singular point on arc $\overarc{D_1A_2}$, ω-limit set of the unstable manifold at this point can only be a itself (bypass the origin and return to A_2 again, forming a homoclinic orbit), C_2 and a singular point on arc $\overarc{D_2C_2}$, respectively. According to the symmetry of the original system, the global phase portraits are equivalent to Figure 1.1 (25), (26) and (27), respectively.

Figure 2.9 (2): Consider the unstable manifold at point C_1, there are three possibilities for the ω-limit set on point C_1, which are a singular on the arc $\overarc{D_1A_2}$, A_2 and C_2. When the ω-limit set of an unstable manifold at C_1 is a singular point on arc $\overarc{D_1A_2}$, ω-limit set of the unstable manifold at this point can only be a itself (bypass the origin and return to A_2 again, forming a homoclinic orbits), C_2 and a singular point on arc $\overarc{D_2C_2}$, respectively. According to the symmetry of the original system, the global phase portraits are equivalent to the Figure 1.1 (29), (28) and (26), respectively.

Figure 2.9 (3): Consider the point A_2, the ω-limit set of the unstable manifold at this point can only be a itself (bypass the origin and return to A_2 again, forming a homoclinic orbit). The α-limit set of the stable manifold at point C_1 can only be a singular on the arc $\overgroup{A_1B_1}$. The ω-limit set of the unstable manifold at point C_1 can only be a singular on the arc $\overgroup{D_1A_2}$. According to the symmetry of the original system, the global phase portrait is equivalent to the Figure 1.1 (30).

Figure 2.9 (4): Consider the point C_1, the ω-limit set of the unstable manifold at this point can only be a singular on the arc $\overgroup{D_1A_2}$. The α-limit set of the stable manifold at point C_1 can only be a singular on the arc $\overgroup{A_1B_1}$. According to the symmetry of the original system, the global phase portrait is equivalent to the Figure 1.1 (27).

Figure 2.9 (5): Consider the point C_1, α-limit set of the unstable manifold at this point can only be a singular on the arc $\overgroup{A_1B_1}$. Based on the the symmetry, ω-limit set of the unstable manifold at the point C_2 can only be a a singular on the arc $\overgroup{A_1B_2}$. Fixed the unstable manifold of C_1, there are three possibilities for the ω-limit set on the C_1 , which are a singular on the arc $\overgroup{D_1A_2}$, A_2 and C_2. Then the global phase portraits are equivalent to the Figure 1.1 (30) (29) (27).

Therefore, the local phase portraits Figure 2.8 have 6 possible global phase portraits as shown in Figure 1.1 (25)–(30).

For case (a.2): $a_2 \neq 0$, $4(a_5 - a_6) < a_2^2$, the local phase portrait of P_1 and P_2 of the system (2.2) consists of one hyperbolic and one elliptic sector by using blowing up. Moving P_1 to the origin through the change of coordinates $(u, v) \mapsto (u + \sqrt{-a_6/a_5}, v)$, the system (2.2) becomes

$$
\begin{cases}
u' = [1 + (u + 2^2)]v^3, \\
v' = uv^4 + \sqrt{-\dfrac{a_6}{a_5}}v^4 - a_1v^3 - a_2uv^2 - a_2\sqrt{-\dfrac{a_6}{a_5}}v^2 - 2a_4\sqrt{-\dfrac{a_6}{a_5}}uv \\
\quad - a_4u^2v - a_5u^3 - 3a_5\sqrt{-\dfrac{a_6}{a_5}}u^2 + 2a_6u.
\end{cases}
\tag{2.10}
$$

We apply a (2,1)-blow up to the system (2.1), and the local phase portrait of point P_1 in the system (2.1) is shown in Figure 2.10 (1). By the same argument, the local phase portrait of point P_2 in the system (2.1) is shown in Figure 2.10 (2). In the chart U_2, we have the same results as the Case IV.
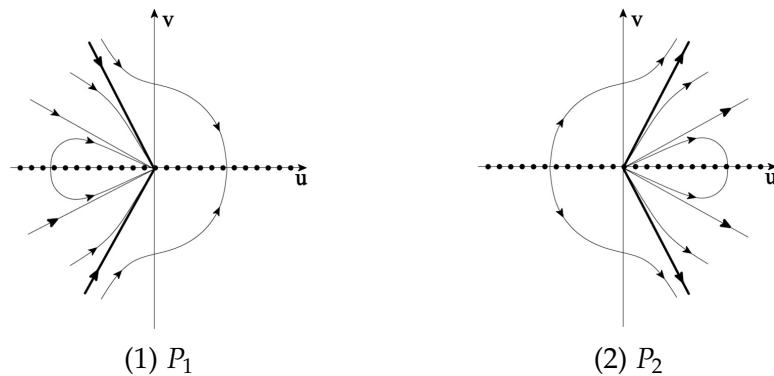

(1) P_1　　　　　　(2) P_2

Figure 2.10: Local phase portrait of system (2.1) at point P_1 and point P_2 . The horizontal axis is filled with singular points.

After the analysis of case (a.2): $a_2 \neq 0$, $4(a_5 - a_6) < a_2^2$, we characterize the local phase portrait of system (1.3) on the Poincaré disk, see Figure 2.11 (1). By the symmetry of the system and the directions of the Poincaré disc, the possible global phase portraits of system (1.3) are shown in Figure 1.1 (31)–(46) of Theorem 1.2.

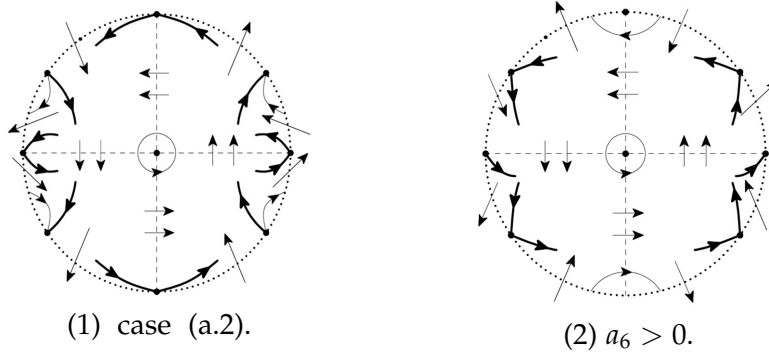(1) case (a.2).   (2) $a_6 > 0$.

Figure 2.11: Local phase portrait of system (1.3) on the Poincaré disk of Case IV.

Using the similar argument as previous cases, if $a_6 > 0$, the local phase portrait of system (1.3) is Figure 2.11 (2), then the global phase portraits in the Poincaré disk are Figure 1.1 (47)–(51).

For Case IV, the possible global phase portrait of system (1.3) is shown in Figure 1.1 (25)–(51) of Theorem 1.2.

Case V: $a_4 a_6 - a_5 \neq 0$, $a_5 a_6 < 0$.

In the chart U_1, we consider the system (2.2). It is easy to find that there are three singular points in the u-axis: $O_{U_1}(0,0)$, $P_1(\sqrt{-a_6/a_5}, 0)$ and $P_2(\sqrt{-a_6/a_5}, 0)$. For the point $O_{U_1}(0,0)$, its singular point is the same to the system (2.2), please refer to Case II(i) and (ii) for details.

For the points P_1 and P_2, their linear part is

$$\begin{pmatrix} 0 & 0 \\ 2a_6 & \frac{a_4 a_6 - a_5}{a_5} \end{pmatrix}.$$

If $a_4 a_6 - a_5 \neq 0$, we have the following statements hold.

(A.1) If $a_6 < 0$ and $a_4 a_6 - a_5 > 0$, then P_1 and P_2 are unstable nodes.

(A.2) If $a_6 < 0$ and $a_4 a_6 - a_5 < 0$, then P_1 and P_2 are stable nodes.

(A.3) If $a_6 > 0$, then P_1 and P_2 are saddles.

In the chart U_2 the origin is the only one singular point of system (2.4). By the same argument as the Case III, if $a_6 < 0$, then the origin is a saddle, and if $a_6 > 0$, then the origin is a center.

Based on the above analysis, we characterize the local phase portrait of system (1.2) on the poincaré disk. If $a_6 > 0$, it is shown in Figure 2.11 (2); if $a_6 < 0$, Case (A.1) and Case (A.2) are equivalent to Figure 2.12.
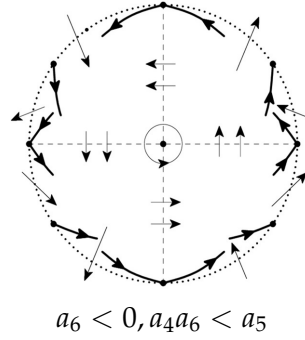
$$a_6 < 0, a_4 a_6 < a_5$$

Figure 2.12: Local phase portrait of system (1.3) on the Poincaré disk of Case (A.1) and (A.2).

By the same argument as Figure 2.8, the possible global phase portraits of Figure 2.12 are Figure 1.1 (52)–(66). For Case IV, the possible global phase portraits of Figure 2.11 (2) are Figure 1.1 (47)–(51).

Therefore, the possible global phase portraits of Case V of system (1.3) are Figure 1.1(47)-(66).

2.2 Global phase portraits of system (1.4)

In this section, we discuss the global phase portraits of system (1.4). For $a_6 = 0$, $a_5 \neq 0$, the global phase portraits of system (1.4) has been studied in [2], thus we only investigate the following situations.

Case i: $a_5 = 0$, $a_6 \neq 0$.

In the chart U_1, the origin $O_{U_1}(0,0)$ of system (2.2) is a singular point and its linear part is

$$\begin{pmatrix} 0 & 0 \\ -a_6 & 0 \end{pmatrix}.$$

By the Theorem 3.5 of [14], if $a_6 < 0$, then $O_{U_1}(0,0)$ is a saddle, and if $a_6 > 0$, then $O_{U_1}(0,0)$ is a center.

In the chart U_2, the origin $O_{U_2}(0,0)$ is the only one singular point of system (2.4). Due to in the chart U_2, the coefficient a_3 does not work, the conclusion of system (1.4) is same to system (1.3), as shown Case II.1 and Case II.2 in Section 2.1.

Based on the above analysis, the corresponding local and global phase portraits of system (1.4) in Case I can be summarized as follows:

i.1 $a_4 = 0$. If $a_6 > 0$, the local phase portrait of system (1.4) on the Poincaré disk is Figure 2.3, but it needs to be rotated $\pi/2$ clockwise rotation, and all possible global phase portraits are topologically equivalent to Figure 1.1 (6) and (22). If $a_6 < 0$, the local phase portrait of system (1.4) is Figure 2.5(a) and Figure 2.3, and all possible global phase portrait is Figure 1.1 (7)–(12) and (6).

i.2 $a_4 \neq 0$. If $a_6 > 0$, the local phase portrait of system (1.4) on the Poincaré disk is Figure 2.13, all possible global phase portraits are topologically equivalent to Figure 1.1 (23) and (24). If $a_6 < 0$, the local phase portrait of system (1.4) is Figure 2.7 (3), and all possible global phase portraits are Figure 1.1 (19)–(21).
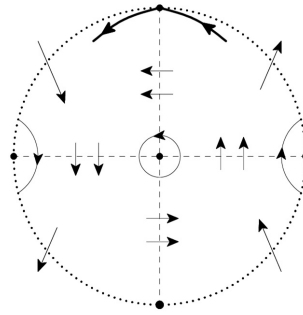
Figure 2.13: Local phase portrait of system (1.4) on the Poincaré disk of Case i.2
for $a_6 > 0$.

Therefore, the system (1.4) has 13 possible global phase portraits in Case i, as shown in
Figure 1.1 (6)–(12) and (19)–(24).

Case ii: $a_5 a_6 > 0$.

If $a_6 > 0$, the local phase portrait of system (1.4) on the Poincaré disk is Figure 2.3, but it
needs to be rotated $\pi/2$ clockwise rotation, all possible global phase portraits are topologically
equivalent to Figure 1.1 (6) and (22). If $a_6 < 0$, the local phase portrait of system (1.4) is Figure
2.3, and all possible global phase portrait is Figure 1.1(6).

Therefore, the system (1.4) has 2 possible global phase portraits in Case ii, as shown in
Figure 1.1 (6) and (22).

Case iii: $a_5 a_6 < 0$, $a_4 \neq 0$.

If $a_6 > 0$, the local phase portrait of system (1.4) on the Poincaré disk is Figure 2.14, all possible
global phase portraits are topologically equivalent to Figure 1.1 (29) and (67). If $a_6 < 0$, the
local phase portrait of system (1.4) is Figure 2.12, and all possible global phase portraits are
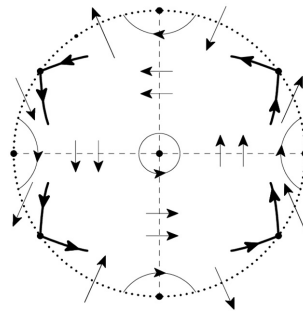Figure 1.1 (52)–(66).

Figure 2.14: Local phase portrait of system (1.4) on the Poincaré disk of Case iii
for $a_6 > 0$.

Therefore, the system (1.4) has 17 possible global phase portraits in Case iii, as shown in
Figure 1.1 (29) and (52)–(67).

Case iv: $a_5 a_6 < 0$, $a_4 = 0$.

If $a_6 > 0$, the local phase portrait of system (1.4) is same to Case iii: $a_6 > 0$, as shown in
Figure 2.14, its corresponding all possible global phase portraits are Figure 1.1 (29) and (67). If
$a_6 < 0$, the local phase portrait of system (1.4) is same to Case IV: $a_6 < 0$, as shown in Figure

2.8 and Figure 2.11 (1), and its corresponding all possible global phase portraits are Figure 1.1 (25)–(30) and (31)–(46).

Consequently, the system (1.4) has 22 possible global phase portraits in Case iv, as shown in Figure 1.1 (25)–(46) and (67).

To sum up, the system (1.2) has 67 possible global phase portraits.

This completes the proof of Theorem 1.2.

Acknowledgements

References

[1] A. Algaba, M. Reyes, Characterizing isochronous points and computing isochronous sections, *J. Math. Anal. Appl.* **355**(2009), 564–576. https://doi.org/10.1016/j.jmaa.2009.02.007; MR2521734; Zbl 1208.34034

[2] A. Algaba, M. Reyes, A. Bravo, Uniformly isochronous quintic planar vector fields, in: *nternational Conference on Differential Equations, Vol. 1, 2 (Berlin, 1999)*, World Scientific Publishing Co., Inc., River Edge, NJ, 2000, pp. 1415–1417. https://doi.org/10.1142/9789812792617_0264; MR1870340; Zbl 0976.37026

[3] A. Algaba, M. Reyes, T. Ortega, A. Bravo, Campos cuárticos con velocidad angular constante, in: *Actas: XVI CEDYA Congreso de Ecuaciones Diferenciales y Aplicaciones, VI CMA Congreso de Matemática Aplicada, Vol. 2*, Las Palmas de Gran Canaria, 1999, pp. 1341–1348.

[4] M. Álvarez, A. Ferragut, X. Jarque, A survey on the blow up technique, *Internat. J. Bifur. Chaos* **21**(2011), 3103–3118. https://doi.org/10.1142/S0218127411030416; MR2871964; Zbl 1258.34001

[5] J. Artés, J. Itikawa, J. Llibre, Uniform isochronous cubic and quartic centers: revisited, *J. Comput. Appl. Math.* **313**(2017), 448–453. https://doi.org/10.1016/j.cam.2016.09.018; MR3573254; Zbl 1355.34054

[6] M. Brunella, M. Miari, Topological equivalence of a plane vector field with its principal part defined through Newton polyhedra, *J. Differential Equations* **85**(1990), 338–366. https://doi.org/10.1016/0022-0396(90)90120-E; MR1054553; Zbl 0704.58038

[7] L. Cairó, J. Llibre, Phase portraits of quadratic polynomial vector fields having a rational first integral of degree 2, *Nonlinear Anal.* **67**(2007), 327–348. https://doi.org/10.1016/j.na.2006.04.021; MR2317173; Zbl 1189.34065

[8] J. Chavarriga, M. Sabatini, A survey of isochronous centers, *Qual. Theor. Dyn. Syst.* **1**(1999), 1–70. https://doi.org/10.1007/BF02969404; MR1747197

[9] T. Chen, S. Li, J. Llibre, Z_2-equivariant linear type bi-center cubic polynomial Hamiltonian vector fields. *J. Differential Equations* **269**(2020), 839–861. `https://doi.org/10.1016/j.jde.2019.12.020`; MR4081537; Zbl 1471.37056

[10] A. Choudhury, P. Guha, On commuting vector fields and Darboux functions for planar differential equations, *Lobachevskii J. Math.* **34**(2013), 212–226. `https://doi.org/10.1134/S1995080213030049`; MR3095726; Zbl 1288.34031

[11] B. Coll, A. Ferragut, J. Llibre, Phase portraits of the quadratic systems with a polynomial inverse integrating factor, *Internat. J. Bifur. Chaos* **19**(2009), 765–783. `https://doi.org/10.1142/S0218127409023299`; MR2533481; Zbl 1167.34324

[12] C. Collins, Conditions for a center in a simple class of cubic systems, *Differential Integral Equations* **10**(1997), 333–356. `https://doi.org/10.57262/die/1367526341`; MR1424815; Zbl 0894.34022

[13] R. Conti, Uniformly isochronous centers of polynomial system in $\mathbb{R}^2$, in: *Differential equations, dynamical systems, and control science*, Lect. Notes Pure Appl. Math., Vol. 152, 1994, pp. 21–31. MR1243191; Zbl 0795.34021

[14] F. Dumortier, J. Llibre, J. Artés, *Qualitative theory of planar differential systems*, Universitext, Springer-Verlag, 2006. `https://doi.org/10.1006/jmaa.1993.1212`; MR2256001; Zbl 1110.34002

[15] G. Fowles, G. Cassiday, *Analytical mechanics*, Thomson Brooks/Cole, 2005.

[16] M. Han, V. Romanovski, Isochronicity and normal forms of polynomial systems of ODEs, *J. Symb. Comput.* **47**(2012), 1163–1174. `https://doi.org/10.1016/j.jsc.2011.12.039`; MR2926120; Zbl 1248.34046

[17] J. Itikawa, J. Llibre, Limit cycles for continuous and discontinuous perturbations of uniform isochronous cubic centers, *J. Comput. Appl. Math.* **277**(2015), 171–191. `https://doi.org/10.1016/j.cam.2014.09.007`; MR3272173; Zbl 1308.34041

[18] J. Itikawa, J. Llibre, Phase portraits of uniform isochronous quartic centers, *J. Comput. Appl. Math.* **287**(2015), 98–114. `https://doi.org/10.1016/j.cam.2015.02.046`; MR3342019; Zbl 1323.34040

[19] J. Itikawa, J. Llibre, Global phase portraits of uniform isochronous centers with quartic homogeneous polynomial nonlinearities, *Discrete. Contin. Dyn. Syst. Ser. B.* **21**(2016), 121–131. `https://doi.org/10.3934/dcdsb.2016.21.121`; MR3426835; Zbl 1334.34069

[20] J. Llibre, Y. Martínez, C. Vidal, Linear type centers of polynomial Hamiltonian systems with nonlinearities of degree 4 symmetric with respect to the *y*-axis, *Discrete Contin. Dyn. Syst. Ser. B* **23**(2018), 887–912. `https://doi.org/10.3934/dcdsb.2018047`; MR3810100; Zbl 1440.34031

[21] J. Llibre, Y. Martínez, C. Vidal, Phase portraits of linear type centers of polynomial hamiltonian systems with Hamiltonian function of degree 5 of the form $h = h_1(x) + h_2(y)$, *Discrete Contin. Dyn. Syst.* **39**(2019), 75–113. `https://doi.org/10.3934/dcds.2019004`; MR3918166; Zbl 1412.37059

[22] J. Llibre, R. Oliveira, Phase portraits of quadratic polynomial vector fields having a rational first integral of degree 3, *Nonlinear Anal.* **70**(2009), 3549–3560. `https://doi.org/10.1016/j.na.2008.07.012`; MR2502763; Zbl 1171.34035

[23] J. Reyn, *Phase portraits of planar quadratic systems*, Mathematics and its Applications, Vol. 583, Springer, 2007. MR2300603; Zbl 1123.34002

[24] D. Schlomiuk, X. Zhang, Quadratic differential systems with complex conjugate invariant lines meeting at a finite point, *J. Differential Equations* **265**(2018), 3650–3684. `https://doi.org/10.1016/j.jde.2018.05.014`; MR3823981; Zbl 1393.37023

[25] J. Sugie, T. Hara, Classification of global phase portraits of a system of Liénard type, *J. Math. Anal. Appl.* **193**(1995), 264–281. `https://doi.org/10.1006/jmaa.1995.1234`; MR1338512; Zbl 0840.34020

[26] Y. Tian, Y. Zhao, Global phase portraits and bifurcation diagrams for Hamiltonian systems of linear plus quartic homogeneous polynomials symmetric with respect to the *y*-axis, *Nonlinear. Anal.* **192**(2020), 111658, 27 pp. `https://doi.org/10.1016/j.na.2019.111658`; MR4023929; Zbl 1442.-37070

[27] Y. Tian, Y. Zhao, Global phase portraits and bifurcation diagrams for reversible equivariant Hamiltonian systems of linear plus quartic homogeneous polynomials, *Discrete. Contin. Dyn. Syst. Ser. B.* **26**(2021), No. 6, 2941–2956, `https://doi.org/10.3934/dcdsb.2020214`; MR4235641; Zbl 1470.34088

[28] K. Wu, Y. Zhao, The cyclicity of the period annulus of the cubic isochronous center, *Ann. Mat. Pura Appl.* **191**(2012), 459–467. `https://doi.org/10.1007/s10231-011-0190-5`; MR2958343; Zbl 1264.34062